The Impedance of a Short Dipole Antenna in a Magnetized Plasma Via a Finite Difference Time Domain Model

Jeffrey Ward, *Student Member, IEEE*, Charles Swenson, *Member, IEEE*, and Cynthia Furse, *Senior Member, IEEE*

***Abstract*—The traditional analytical analysis of plasma probes requires the use of quasi-static approximations, while numerical methods require the use of an equivalent dispersive media, both producing a nontrivial analysis of the plasma environment. On the other hand, a few techniques that combine the plasma fluid equations with Maxwell's equations have only addressed wave propagation through spatially constant plasma. All of these models are limited in analysis of in situ measurements. This paper modifies the current finite-difference time-domain methods to more accurately model the ionospheric environment. Decoupled boundary conditions are presented in an attempt at coping with the instabilities of the plasma at the boundaries. The final model is then compared to analytical theory of radio-frequency plasma probes.**

***Index Terms*—Antenna theory, finite-difference time-domain (FDTD) methods, plasma covered antennas, plasma measurements.**

I. Introduction

THE impedance of an electrically short antenna immersed in plasma has been studied extensively for the last 50 years, both theoretically [1]–[6] and experimentally [7]–[10]. By electrically short, we mean an antenna with small physical dimensions, compared to the free space wavelength at the driving frequency. The plasma antenna interaction has been used as a diagnostic for space plasmas where the impedance characteristics at radio frequencies are a strong function of free electron density. Impedance probes have advantages over Langmuir type probes [11], [12] in that to first order they are insensitive to surface contaminations and vehicle charging effects [8]. However, the full potential of the technique has not been realized due to limitations of analytical theories. In addition to having a good instrument to make accurate measurements, plasma analysis also requires a good theoretical model of the probe physics [13]. In this paper, we present a numerical finite-difference time-domain (FDTD) simulation of a dipole antenna immersed in typical ionospheric plasma and compare the results to a leading analytical theory by Balmain [14]. In this process, we show that assumptions, which make the problem analytically tractable, lead to significant differences with our simulation results where these assumptions are not made.

The analytical theories for the impedance of an electrically short antenna are typically developed in the following manner: the complex power S is computed from the fields around the antenna that are driven by a sinusoidal steady-state current of frequency ω at the antenna inputs. This power is then related to the input impedance $Z(\omega)$ of a lumped element from circuit theory with driving current I_o

$$S(\omega) = \frac{1}{2} I_o^2 Z(\omega). \tag{1}$$

The complex power around the antenna can be computed either by integrating the Poynting vector $\vec{S}$ over a closed surface or by integrating the product of the surface currents and fields $J \cdot E$ over the surface of the antenna

$$S(\omega) = -\oint \vec{S} \cdot \vec{n}\, \mathrm{d}a = \int_S \vec{J}^* \cdot \vec{E}\, \mathrm{d}a. \tag{2}$$

The problem is made analytically tractable by assuming a surface current distribution on the antenna from which fields in (2) are computed. This is called the induced electromotive force (EMF) method. A triangular distribution is commonly used for short dipole antennas [5]. The plasma is modeled as an anisotropic dielectric medium where ϵ_r is given by

$$\epsilon_r = \begin{pmatrix} \epsilon_1 & -j\epsilon_2 & 0 \\ j\epsilon_2 & \epsilon_1 & 0 \\ 0 & 0 & \epsilon_3 \end{pmatrix} \tag{3}$$

with

$$\epsilon_1 = 1 - \frac{\omega_p^2 \left(1 - j\frac{\nu}{\omega}\right)}{\omega^2 \left(1 - j\frac{\nu}{\omega}\right)^2 - \Omega^2} \tag{4}$$

$$\epsilon_2 = -\frac{\omega_p^2 \Omega / \omega}{\omega^2 \left(1 - j\frac{\nu}{\omega}\right)^2 - \Omega^2} \tag{5}$$

$$\epsilon_3 = 1 - \frac{\omega_p^2}{\omega^2 \left(1 - j\frac{\nu}{\omega}\right)} \tag{6}$$

where ν represents the electron-neutral collision frequency, Ω is the electron gyro frequency, and ω_p is the plasma frequency where

$$\Omega = \frac{|e|B}{m} \tag{7}$$

$$\omega_p = \sqrt{\frac{ne^2}{\epsilon_0 m}} \tag{8}$$

which are dependent on the plasma charge (e), density (n), mass (m), and ambient magnetic field (B).

Approximations are used to develop this dielectric model of the plasma from either fluid or kinetic theory [4]. The typical

Manuscript received January 15, 2004; revised January 24, 2005.

The authors are with Utah State University, Logan, UT 84322 USA (e-mail: jward@cc.usu.edu).

Digital Object Identifier 10.1109/TAP.2005.851823

0018-926X/$20.00 © 2005 IEEE

assumption is a high-frequency model where ion dynamics are ignored. Various other assumptions typically made to decrease the complexity of the problem include cold versus warm, collisionless versus collisional, and unmagnetized versus magnetized plasmas. In addition, the analytical computation of the fields around the antenna, even with a proscribed current distribution, typically becomes tractable under a quasi-static assumption. Therefore, the complex power leaving the antenna in the form of electromagnetic and some plasma waves is ignored.

The problem is formulated using sinusoidal steady-state Maxwell's equations with the prescribed current distribution Fourier transformed in the spactial variables k_x, k_y, and k_z. Parsaval's theorem is then used to formulate a generalized equation for the input impedance

$$Z(\omega) = \frac{i}{\omega\epsilon_o(2\pi)^3|I(0)|^2}\int \frac{[\vec{k}\cdot\vec{J}(\vec{k})][\vec{k}\cdot\vec{J}^*(\vec{k})]}{\vec{k}\cdot[\vec{\epsilon}(\vec{k},\omega)\cdot\vec{k}]}d\vec{k}. \quad (9)$$

The solution of this integral equation is complicated by the poles that arise from the natural modes of the plasma $\vec{k}\cdot[\vec{\epsilon}(\vec{k},\omega)\cdot\vec{k}] = 0$. For certain orderings of ω_p and Ω_e in frequency and assumed current distributions, the problem becomes intractable, particularly in the cutoff or nonpropagating frequency regions for electromagnetic (EM) waves, and approximate solutions make the theories suspect. This equation is further complicated when solving for all orientations of the antenna relative to the background magnetic field. A successful general theory for the impedance of an antenna in magnetized plasma has been developed by Balmain [15], [14], [16], for a line current distribution of arbitrary orientation relative to the magnetic field in a cold collisional plasma.

To summarize, the major assumptions and limitations of the closed-form analytical theories for electrically short antenna immersed in plasma are the following.

1) They are limited to dipole or loop configurations where the assumed current distribution along the antenna is simplified, and the resonance effects of the current distribution are assumed to be negligible.
2) This produces a high-frequency sinusoidal steady-state plasma model, ignoring any transient behavior and low-frequency behavior where ion dynamics become important.
3) A cold, linear plasma is assumed, where temperature effects and nonlinear shock-like phenomena are neglected.
4) These theories are limited to a quasi-static model of the electric and magnetic fields, which ignores interactions between the fields and their impact on the antennas impedance, particularly in frequency regions where the antenna is resonant with the plasma.
5) Analytical theories are limited to spatially uniform plasma density distribution, preventing the accurate self-consistent description of plasma sheath effects on antenna impedance.

Computers have increased significantly in power and capability over the last few decades, while decreases in cost make simulation of plasma wave problems far more tractable. A number of FDTD-type simulations of plasmas have been reported in the literature [17]–[24]. However, these models continue to treat the plasma as an anisotropic dielectric and are unable to resolve all of the problems of the analytical theories, namely numbers 3) and 5) from the above list.

The experimental space science community will be aided by a complete theory or model for the interaction of an arbitrary shaped antenna immersed in magnetized space plasma. This would aid the design and interpretation of data from electric field probes, impedance probes, and radio-frequency (RF) sounders on a spacecraft. A reasonable approach to this problem is to develop a straightforward FDTD simulation of the governing equations with appropriate boundary conditions for the antenna and simulation. This paper will describe our model, the plasma fluid FDTD (PF-FDTD) model, which has been developed for this purpose, and compare initial results with the leading analytical theory of Balmain [15], [14], [16].

II. The Model

A. The Equations

The plasma environment can be represented by several different sets of equations, depending on the boundary conditions, the physics in which the individual is interested, and the simplifying assumptions that can be made. By limiting our analysis to measurements on the order of several Debye lengths and treating the ions and neutrals as stationary particles, the simplest model is the subsonic incompressible $((\vec{U}\cdot\nabla)\vec{U} = 0)$ five moment Maxwellian plasma fluid equations [25]. It is composed of three basic equations: the continuity equation

$$\frac{\partial n}{\partial t} + \nabla\cdot(n\vec{U}) = 0 \quad (10)$$

the momentum equation

$$mn\frac{\partial\vec{U}}{\partial t} = nq(\vec{E} + \vec{U}\times\vec{B}_0) - \nabla P + nm\nu(\vec{U} - \vec{V}) \quad (11)$$

and the ideal gas law

$$P = nk_bT \quad (12)$$

where $m, n, q, \vec{U}, T$ represent the mass, density, charge, velocity, and kinetic temperature of electrons, $\vec{E}$ and $\vec{B}$ are the electric field and magnetic flux, ν and $\vec{V}$ are the electron neutral collision rate and neutral velocity respectively, and k_b is the Boltzmann constant. Maxwell's equations are then used to complete the set of ten unknowns and ten equations

$$\nabla\times\vec{E} = -\frac{\partial\vec{B}}{\partial t} \quad (13)$$

$$\nabla\times\vec{B} = \epsilon\mu\frac{\partial\vec{E}}{\partial t} + \mu\vec{J} \quad (14)$$

$$\nabla\times\vec{B} = \epsilon\mu\frac{\partial\vec{E}}{\partial t} + \mu qn\vec{U} \quad (15)$$

with the plasma current $\vec{J} = qn\vec{U}$.

Like all FDTD simulations, the first step is to discretize the equations in space. By placing the density at the center of the Yee cell (see Fig. 1), all particles in the Yee cell can be treated as a single centralized particle. However, if the plasma is allowed to have an initial velocity or spatial density variations that cannot be ignored, such as a charged satellite traversing through the

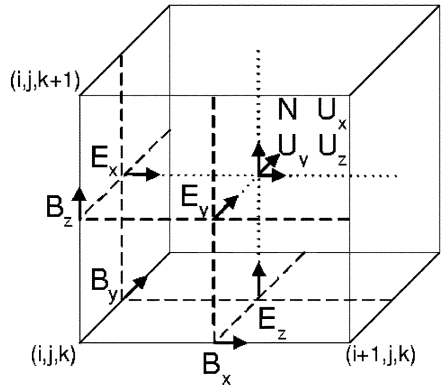

Fig. 1. PF-FDTD cell.

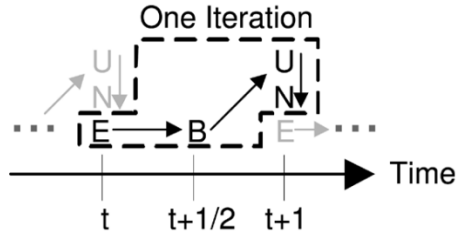

Fig. 2. PF-FDTD leapfrog scheme.

ionosphere, the velocity must then be applied directly to the single particle in order to minimize the spatial averaging in the second term of (10). The electric and magnetic fields are then placed in the standard FDTD locations, as shown in Fig. 1, to complete the set.

Once spatially discretized, the fields must then be temporally discretized (see Fig. 2). The electric and magnetic fields are located at alternating 1/2 time steps, similar to the standard leapfrog FDTD simulation. The temporal location of the velocity can be found by analyzing Ampere's (15), which states that the velocity must be known at the same time step as the magnetic flux. However, as with the spatial discretization, if an initial velocity or spatial variations in density are allowed, the density and velocity must be known at the same point in time in order to minimize the averaging of (10).

When the continuity (10) is solved for N^{t+1}, it becomes

$$\begin{aligned} N^{t+1}(i,j,k) &= N^{t-1}(i,j,k) \\ &\quad - \Delta t \left(N^t(i,j,k) \frac{U_x^t(i+1,j,k) - U_x^t(i-1,j,k)}{2\Delta x} \right. \\ &\quad + U_x^t(i,j,k) \frac{N^t(i+1,j,k) - N^t(i-1,j,k)}{2\Delta x} \\ &\quad + N^t(i,j,k) \frac{U_y^t(i,j+1,k) - U_y^t(i,j-1,k)}{2\Delta y} \\ &\quad + U_y^t(i,j,k) \frac{N^t(i,j+1,k) - N^t(i,j-1,k)}{2\Delta y} \\ &\quad + N^t(i,j,k) \frac{U_z^t(i,j,k+1) - U_z^t(i,j,k-1)}{2\Delta z} \\ &\quad \left. + U_z^t(i,j,k) \frac{N^t(i,j,k+1) - N^t(i,j,k-1)}{2\Delta z} \right). \end{aligned} \tag{16}$$

A similar process can be performed on (11). Equating the vector terms, applying the central difference formula, and solving for U_x^{t+1} gives

$$\begin{aligned} U_x^{t+1/2}(i,j,k) &= U_x^{t-3/2}(i,j,k) \\ &\quad + \frac{q\Delta t}{2m} \left[E_x^t(i,j,k) + E_x^{t-1}(i,j,k) \right. \\ &\quad + E_x^t(i+1,j,k) + E_x^{t-1}(i+1,j,k) \\ &\quad + 4U_y^{t-1/2}(i,j,k)B_0 \\ &\quad \left. + 4U_z^{t-1/2}(i,j,k)B_0 \right] \\ &\quad - k_b T \Delta t \frac{N^t(i+1,j,k) - N^t(i-1,j,k)}{m\Delta x N^t(i,j,k)} \\ &\quad + 2\nu\Delta t U_x^{t-1/2}(i,j,k). \end{aligned} \tag{17}$$

Similar equations are obtained for U_y and U_z.

The discretization of Maxwell's equations is trivial and can be found in many textbooks [26]. However, due to the addition of the plasma current, Ampere's circuit law becomes

$$\begin{aligned} &E_x^t(i,j,k) \\ &\quad = E_x^{t-1}(i,j,k) \\ &\qquad + \frac{\Delta t}{\mu} \left[\frac{B_z^{t-1/2}(i,j+1/2,k) - B_z^{t-1/2}(i,j-1/2,k)}{\Delta y} \right. \\ &\qquad - \frac{B_y^{t-1/2}(i,j,k+1/2) - B_y^{t-1/2}(i,j,k-1/2)}{\Delta z} \\ &\qquad - \frac{\mu q}{4} \left(N^{t-1/2}(i,j,k) + N^{t-1/2}(i-1,j,k) \right) \\ &\qquad \left. \times \left(U_x^{t-1/2}(i,j,k) + U_x^{t-1/2}(i-1,j,k) \right) \right]. \end{aligned} \tag{18}$$

It is the combination of the fluid equations and relocating of the velocity to the center of the Yee cell and aligning it in time with the calculation of density that enable the PF-FDTD to successfully solve the boundary value problem of an antenna in a plasma.

B. Boundary Conditions

Once the FDTD cell is defined, the antenna can be modeled by imposing tangential electric field boundary conditions on the metallic cells. For a dipole, the tangential electric field is set to zero along the length of the antenna, and the perpendicular field is self-consistently calculated. A gap feed can then be used to apply a Gaussian derivative voltage via Gauss's law, while the current can be monitored using Ampere's law [26]. By combining Ohm's law and the Fourier transform, it is possible to convert the temporal voltage and current into the impedance verses frequency characteristics of an antenna.

Like all numerical simulations, the limitations in memory size force the PF-FDTD model to be truncated. Many absorbing boundary conditions have been developed for FDTD simulations, ranging from retarded time absorbing boundary to perfectly matched layers [27], [28], all of which assume wave propagation at or near the speed of light. However, since many wave

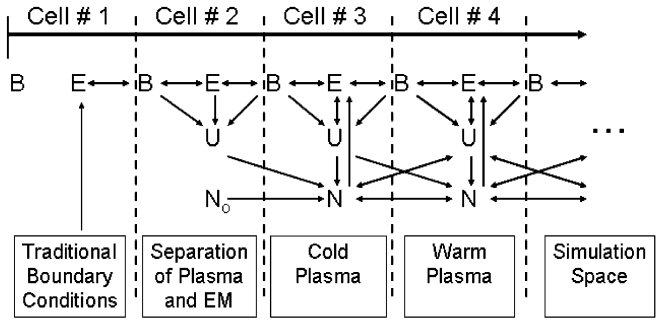

Fig. 3. Interdependency of fields for different spatial locations near the PF-FDTD boundary.

modes, with various propagation speeds, can exist in magnetized plasma, care must be taken when dealing with the sharp gradients near the simulation edge. Previous attempts at apply the retarded time absorbing boundary conditions to both the plasma and electric field had mixed results, and are likely to be the leading cause of instabilities in Olakangil's model [29].

To overcome some of the instabilities associated with applying traditional boundary conditions to the plasma, a boundary condition to decouple the plasma from the electromagnetic waves near the boundary is developed. This is done by decreasing the simulation size of the plasma's velocity and density, similarly to the magnetic field calculations in the traditional FDTD simulation. As shown in Fig. 3, when appropriate boundary conditions, such as retarded time absorbing boundary conditions, are applied to the electric field, the magnetic field in the adjacent cell sees an effective "infinite space." By analyzing the momentum (11) for a cold plasma ($\nabla P = 0$), the velocity will see "infinite space" as long as the magnetic and electric fields in the same cell see "infinite space." The density, however, requires the knowledge of the velocity and density in the adjacent cell. By stepping the plasma away from the edge of the simulation, as seen in Fig. 3, it becomes possible to model a cold collisional plasma as long as the density at the boundary remains constant. This is a safe assumption as long as any low-power source is several Debye lengths away from the edge. Depending on which region of the ionosphere you are modeling, this can be anywhere from centimeters to meters, as shown in Fig. 4. As the power of the probe increases, so must the simulation space, in order to maintain a constant density at the boundary.

To simulate warm plasma, the density must be known in all neighboring cells, due to the gradient of $n(\nabla P = k_b T \nabla n)$. Ideally, this could be calculated up to the separation of the EM fields from the plasma. However, since the boundaries are positioned to maintain a constant density at the edge, there are no temperature effects seen until the density is allowed to vary. As such, to decrease computational load the warm plasma ($\nabla P \neq 0$) is phased into the simulations after the cold plasma has been added, and the density becomes a variable, as shown in Fig. 3.

This is a good boundary condition for energy traveling near the speed of light, but it only addresses half of the problem. The energy in the slower moving waves must also be dissipated at the boundaries. However, to date, we have not developed an effective way of dealing with this energy. Instead the edges of

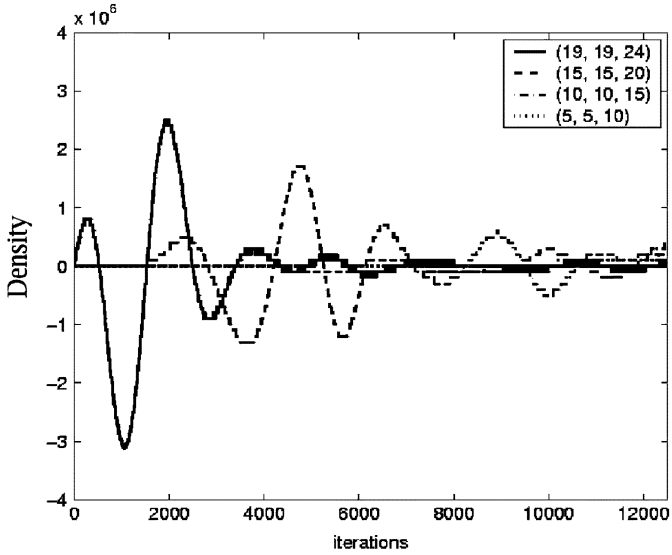

Fig. 4. Variations in density for various locations. (Source is located at [20 20 25]).

the simulations are placed "far" enough so while the traditional Courant condition

$$\Delta t \leq \frac{\Delta x}{\sqrt{3}c} \tag{19}$$

is met, several plasma cycles (tens of thousands of iterations) may be run before the slow moving energy is reflected and returns to corrupt the source data, as shown in Fig. 5.

III. Simulation Results

The PF-FDTD simulation is validated by comparison with the analytical theory of Balmain [14]. This is done by modeling a 1-m dipole antenna in uniform cold, collisional plasma. While it is possible to provide an exhaustive analysis, this paper will only focus on two general cases: one for the antenna parallel and one for the antenna perpendicular to the magnetic field. For each of these two cases, three different orderings of the plasma and gyro frequencies are explored: $\omega_p > \Omega, \omega_p = \Omega, \omega_p < \Omega$. These are the same conditions treated by Balmain [14]. The simulation is set up with a cold plasma of density of approximately 1×10^{12} electrons/m^3 and a collision frequency of $0.1\omega_p$. Under these conditions, Fig. 5 shows that the boundaries must be at least 20 cells away from the antenna to provide sufficient simulation time before the slow-moving waves corrupt the simulation. A simulation size of [70 70 65] was used to maximize the resolution of the antenna within the simulation and to ensure that the constant density approximation at the boundaries was valid. The spatial resolution of the simulations was $\mathrm{dx} = \mathrm{dy} = \mathrm{dx} = 0.04$ m while the temporal resolution was $\mathrm{dt} = 6.67 \times 10^{-11}$ s. All simulations were successfully run for at least 24 plasma periods or approximately 36 000 time steps.

In the comparison of the PF-FDTD to Balmain, two complexities immediately surfaced. The first deals with the ratio of length to diameter or (l/a) of the antenna. The l/a ratio for the simulation was found by computing the free space impedance of the antenna and comparing with Johnson [30]. This was done by running the simulation with no plasma or $\omega_p = 0$. Thus only

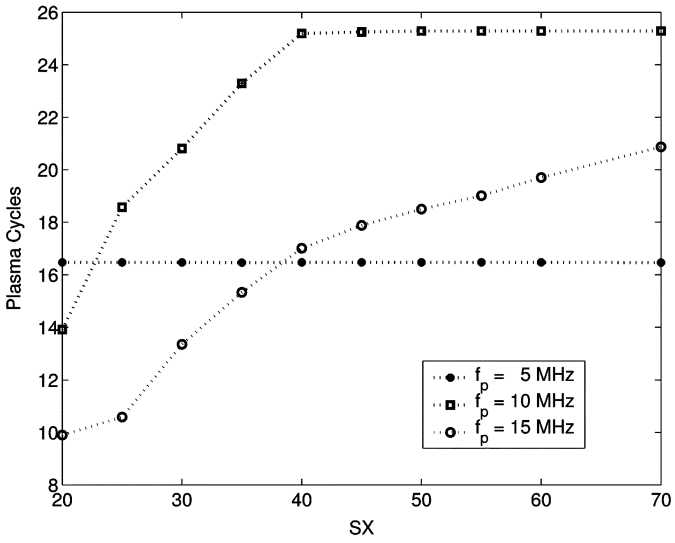

Fig. 5. Number of plasma cycles simulated before the slow moving energy is reflected and corrupts the source data as a function of simulation size for various plasma parameters with a fixed source frequency bandwidth.

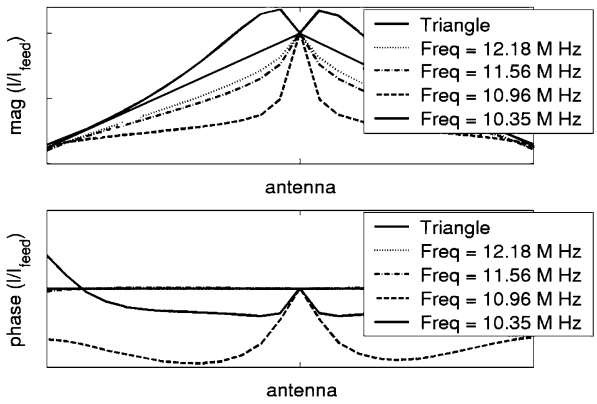

Fig. 6. Current distribution along a dipole antenna for frequencies near the upper hybrid ($\omega_{uh} = 11$ MHz).

electromagnetic wave physics were simulated. An effective l/a of 200 was found for the 1-m antenna in the given simulation grid.

The second complexity is that the PF-FDTD self-consistently computes surface current distribution while Balmain's theory is based on the induced EMF method. Thus the current distributions can be significantly different in the more complete PF-FDTD simulation. The current distribution along the antenna was found to be triangular at frequencies away from fundamental plasma frequencies, while the current distributions at frequencies near ω_{uh} (Fig. 6) are more exponential in nature. The variations in the current distribution are expected as energy is more efficiently coupled into the plasma at resonances [25]. These observations are also in agreement with the experimental data of Ishizon [31] in which the measured distribution showed similar responses. While this dramatic variation does not yield significant qualitative differences, as shown by our results and by closed-form theory [5], it can explain why experimental data have never yielded the high impedance values near the resonances as predicted by Balmain [32].

A. Cold Collisional Magnetized Plasma With Probe Parallel to the DC Magnetic Field

Under sinusoidal steady-state conditions, energy input to an electrically short antenna can be reactively coupled into the plasma, dissipated through heating, or radiated away. The reactive coupling strength is determined by the reactance of the antenna impedance, while the energy lost to heating or radiation contributes to the resistive component. Electrons circulate around magnetic field lines at the gyro frequency and therefore easily transport energy away from an antenna through waves or local heating at this frequency. This shows up as a reduction in the free space conditions of the resistive component at the gyro frequency. Conversely, at the plasma frequency, the electrons are not transporting energy away from the antenna, resulting in a highly reactive component that translates into a large resistive part. All of these can be qualitatively observed in Fig. 7.

Fig. 7 also shows a comparison between Balmain and the PF-FDTD for an antenna aligned with the magnetic field. Qualitatively, there is good agreement between the theories above $0.3\omega_p$. The errors below $0.3\omega_p$ are due to the lack of data points available for the fast Fourier transform (FFT) and the fact that Balmain does not account for the additional physics that occur in plasma outside of the three primary resonances. While this model attempts to provide a method of modeling the additional physics in this region, the simulation must be run for more iterations in order to collect the necessary data points for the FFT at those frequencies. This means either a large simulation space or boundary conditions that are more effective for the slow moving waves are needed.

Above $0.3\omega_p$, the differences between Balmain and the PF-FDTD model are harder to account for and become more an argument for one approach over another. At first glance, the fact that the PF-FDTD does not match Balmain for the same l/a raises questions. However, Balmain has only been experimentally validated for frequencies at the gyro frequency and for frequencies above the upper hybrid [33], due largely to the quasistatic approximations. The PF-FDTD matches Balmain around the gyro frequency and approaches the free space values faster then Balmain for frequencies above the upper hybrid. In the other regions, the PF-FDTD agrees with a smaller l/a ratio, as expected given the exponential nature of the current distribution, as shown in Fig. 6.

Care must also be taken if this method is to be used in a "total" frequency analysis of the antenna, as the numerical representation of a Gaussian derivative source has a limited bandwidth. Analysis of frequencies outside of this bandwidth will allow roundoff errors to corrupt the data. This is why no graphs presented in this paper have included the "free space" response of the antenna above the upper hybrid frequency.

Additional simulations have also shown the correct damping of the resonances as the collision frequency is increased, due to the added energy lost during electron/neutral collisions. The model also demonstrates that the zero phase crossing is offset by the free space capacitance. This raises concern that RF probes used for space plasma diagnostics that only track the zero crossing of the upper hybrid may yield an unrealistically

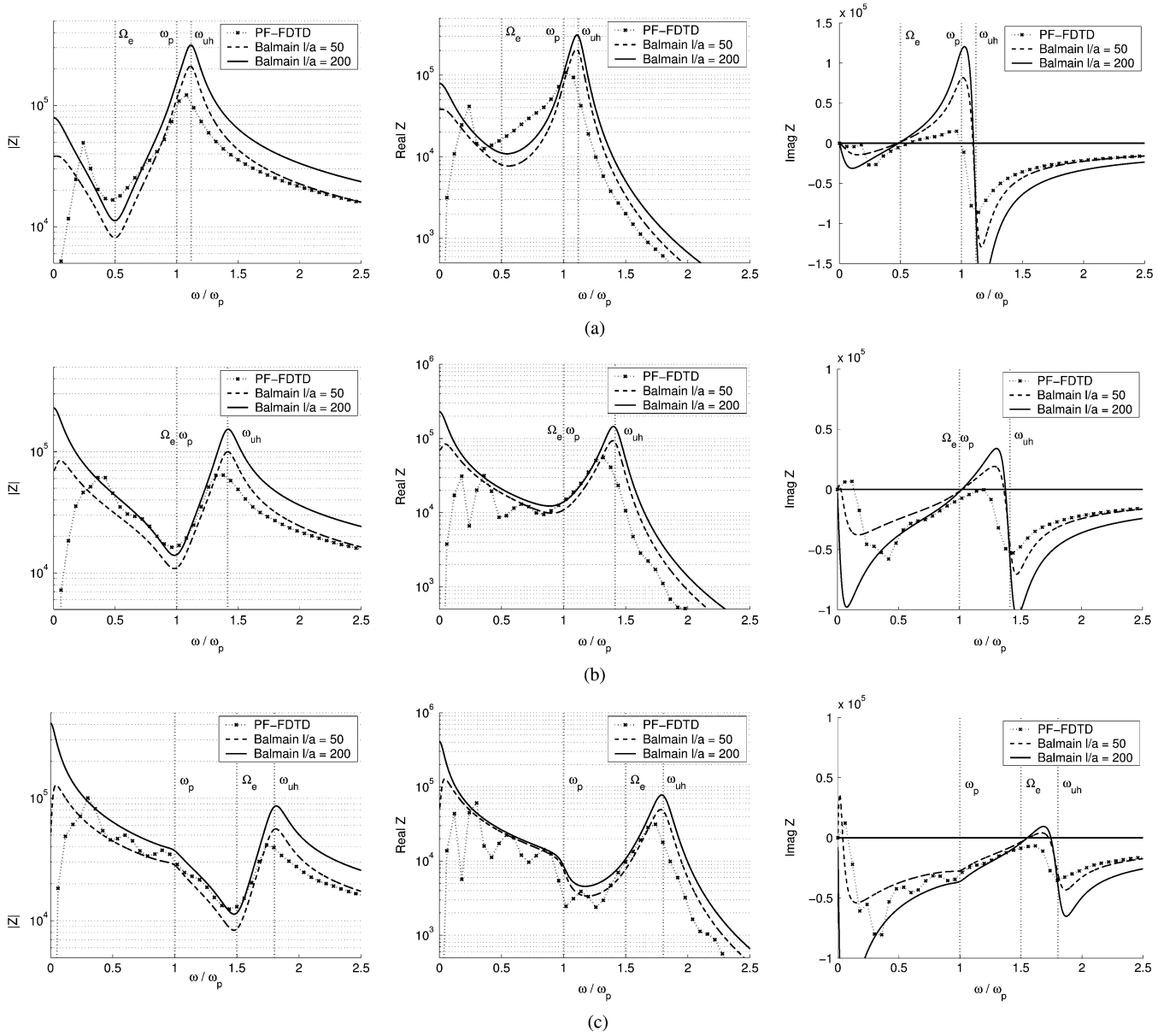

Fig. 7. Input impedance versus frequency for an RF probe with a parallel magnetic field in cold collisional plasma. (a) Gyro frequency $<$ plasma frequency, (b) gyro frequency $=$ plasma frequency, and (c) gyro frequency $>$ plasma frequency.

low plasma density. To correct this problem the free space capacitance must be subtracted from the final measurement.

B. Cold Collisional Magnetized Plasma With Probe Perpendicular to the DC Magnetic Field

As the incident angle of the magnetic field is changed, the effective coupling area that the antenna presents to the different resonant frequencies changes. As the current flows along the antenna, the free electrons in the plasma will mirror the movement. As such, when the antenna is aligned with the magnetic field, the movement of electrons near the antenna is along the field lines. Thus, the gyro frequency is emphasized, and effects of the plasma frequency are minimized. When the antenna is placed perpendicular to the magnetic field, the opposite occurs, as can be seen by comparing the results when the gyro frequency is greater then the plasma frequency in Figs. 7 and 8.

In addition to showing reasonable agreement between Balmain and the PF-FDTD for an incident magnetic field, subject to the variations between theories being explained by similar arguments as presented in the above section, Fig. 8 also presents an unusual side effect of increasing the antenna coupling with the plasma frequencies. Traditionally the RF probes have been flown in regions where the plasma frequency is greater then the gyro frequency, thus easing data analysis of plasma densities, since the upper hybrid converges to the plasma frequency. However, if the plasma frequency is less then the gyro frequency, such as from 80–20 km in the ionosphere or in the solar wind, it is still possible to obtain a prominent feature in the characteristic curve at the plasma frequency. Thus if an RF probe sweeps frequencies as opposed to just tracking the resonances, it becomes possible to measure plasma densities regardless of the plasma/vehicle conditions.

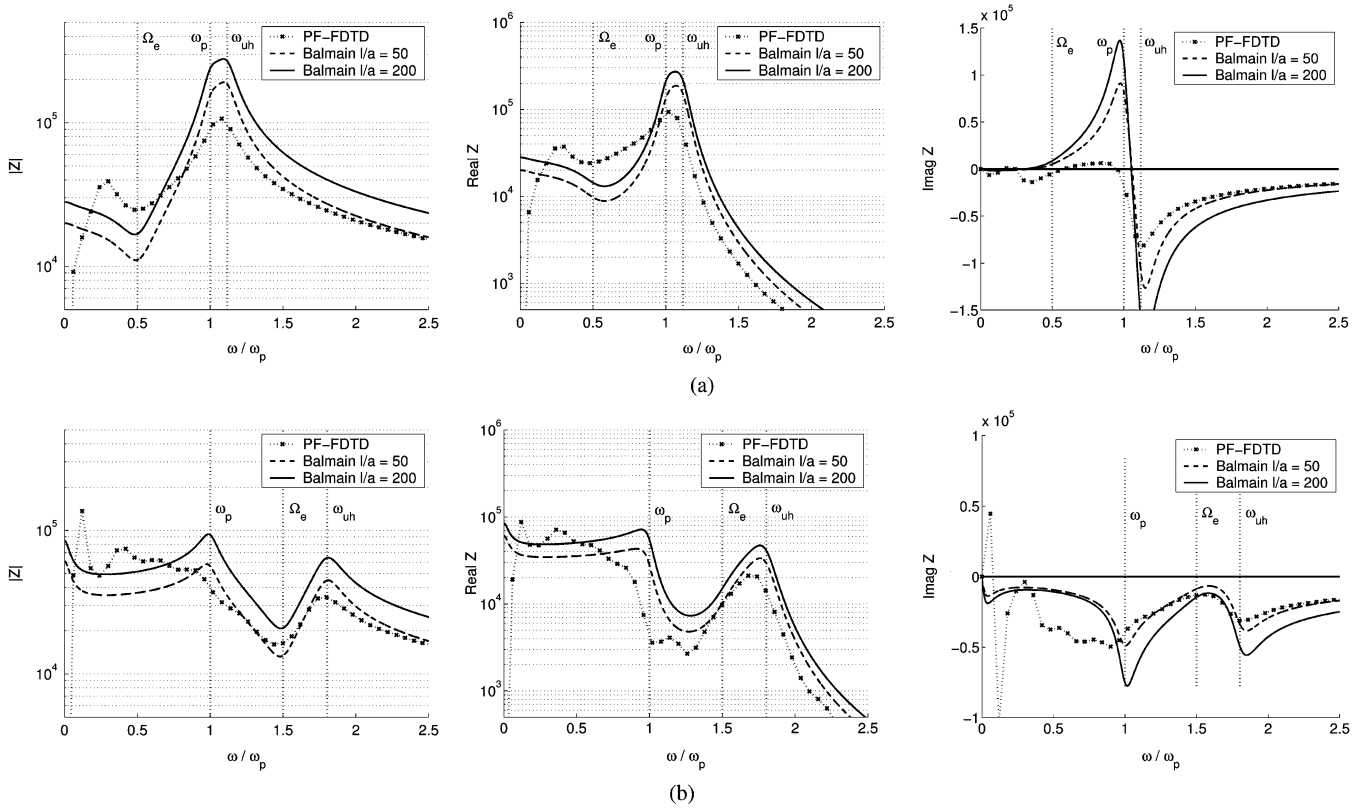

Fig. 8. Input impedance versus frequency for an RF probe with an incident magnetic field in cold collisional plasma. (a) Gyro frequency $<$ plasma frequency and (b) gyro frequency $>$ plasma frequency.

IV. Conclusion

This paper presented a new approach to the important analysis of the impedance of an antenna in plasma. The ability to more accurately model the antenna–plasma interaction enables RF probes to measure plasma parameters to a new level of accuracy. While traditional theories predicted high Qs for the upper hybrid resonance, the PF-FDTD predicts a lower Q. This discrepancy is due to the simplified assumed current distributions of the analytical theories which are nonphysical under resonance conditions.

In addition, the fact that the zero crossing of the upper hybrid resonance shifts negative as the free space capacitance increases will require a redesign of the current probe technique to subtract the free space capacitance before the density measurements are made. However, assuming that some of the emanating field lines traverse undisturbed plasma, the RF probe could take a measurement well above the upper hybrid. This effective free space and sheath-affected capacitance could then be subtracted out of the data. This, combined with the ability to measure very low plasma densities, enables the RF probes to operate under conditions where Langmuir probes fail.

There may be times when the simplicity and ease of the analytical methods may be more desirable than spending the time required to analyze an antenna via the PF-FDTD for varying plasma conditions. While the current limitations of boundary conditions limit the PF-FDTD, many doors are still opened that could not have been imagined with analytical theories. The ability to overcome the current limitations of modeling the effects of plasma temperature, drifts, and density variations, enable the PF-FDTD to become the first numerical model that can accurately represent the antenna plasma interaction on board a satellite or sounding rocket.

References

[1] C. C. Bantin and K. G. Balmain, "Monopole and dipole antennas in a nonlinear isotropic plasma," *Can. J. Phys.*, vol. 52, no. 4, pp. 302–317, Feb. 1974.

[2] J. Galejs, "Impedance of a finite insulated cylindarical antenna in a cold plasma with a longitudinal magnetic field," *IEEE Trans. Antennas Propag.*, vol. AP–14, no. 6, pp. 727–736, Nov. 1966.

[3] M. A. Matin, K. Sawaya, T. Ishizone, and Y. Mushiake, "Impedance of a monopole antenna over a ground plane and immersed in a magneto-plasma," *IEEE Trans. Antennas Propag.*, vol. AP–28, no. 5, pp. 332–341, May 1980.

[4] D. T. Nakatani and H. H. Kuehl, "Input impedance of a short dipole antenna in a warm anisotropic plasma, 1, kinetic theory," *Radio Sci.*, vol. 11, no. 5, pp. 433–444, 1976.

[5] P. Nikitin and C. Swenson, "Impedance of a short dipole antenna in a cold plasma," *IEEE Trans. Antennas Propag.*, vol. 49, no. 10, pp. 1377–1381, Oct. 2001.

[6] H. Staras, "The impedance of an electric dipole in a magneto-ionic medium," *IEEE Trans. Antennas Propag.*, vol. AP–12, no. 6, pp. 695–702, Nov. 1964.

[7] J. E. Jackson and J. A. Kane, "Measurement of ionospheric electron densities using an rf probe technique," *J. Geophys. Res.*, vol. 64, no. 8, pp. 1074–1075, Aug. 1959.

[8] M. D. Jensen and K. D. Baker, "Measuring ionospheric electron density using the plasma frequency probe," *J. Spacecraft Rockets*, vol. 29, no. 1, pp. 91–95, Jan.–Feb. 1992.

[9] C. T. Seigies, D. Block, M. Hirt, B. Hipp, A. Piel, and J. Grygorczuk, "Development of a fast impedance probe for absolute electron density measurements in the ionosphere," *J. Phys. D Appl. Phys.*, vol. 33, pp. 405–413, 2000.

[10] E. J. Lund, M. L. Trimpi, E. H. Gewirtz, R. H. Cook, and J. LaBelle, "The plasma frequency tracker: An instrument for probing the frequency structure of narrow-band mf/hf electric fields," in *Measurements Techniques in Space Plasmas: Fields*, R. F. Pfaff, Ed. Washington, DC: American Geophysical Union, 1998.
[11] H. M. Mott-Smith and I. Langmuir, "The thoery of collectors in gaseous," *Phys. Rev.*, vol. 28, p. 727, 1926.
[12] L. H. Brace, "Langmuir probe measurements in the ionosphere," in *Measurements Techniques in Space Plasmas: Particles*, R. F. Pfaff, Ed. Washington, DC: American Geophysical Union, 1998.
[13] L. R. Storey, "What's wrong with space plasma metrology?," in *Measurements Techniques in Space Plasmas: Particles*, R. F. Pfaff, Ed. Washington, DC: American Geophysical Union, 1998.
[14] K. G. Balmain, "Dipole admittance for magnetoplasma diagnostics," *IEEE Trans. Antennas Propag.*, vol. AP-17, no. 3, pp. 389–392, May 1969.
[15] ——, "The impedance of a short dipole antenna in a magnetoplasma," *IEEE Trans. Antennas Propag.*, vol. AP–12, no. 5, pp. 605–617, Sep. 1964.
[16] ——, "The properties of antennas in plasmas," *Ann. Telecommmun.*, vol. 35, no. 3–4, pp. 273–283, Mar.–Apr. 1979.
[17] S. A. Cummer, "An analysis of new and existing FDTD methods for isotropic cold plasma and a method for improving their accuracy," *IEEE Trans. Antennas Propag.*, vol. 45, no. 3, pp. 392–400, Mar. 1997.
[18] F. Hunsberger, R. Luebbers, and K. Kunz, "Finite-difference time-domain analysis of gyrotropic media—I: Magnetized plasma," *IEEE Trans. Antennas Propag.*, vol. 40, no. 12, pp. 1489–1495, Dec. 1992.
[19] J. H. Lee and D. K. Kalluri, "Three-dimensional FDTD simulation of electromagnetic wave transformation in a dynamic inhomogeneous magnetized plasma," *IEEE Trans. Antennas Propag.*, vol. 47, no. 7, pp. 1146–1151, Jul. 1999.
[20] R. J. Luebbers, F. Hunsberger, and K. S. Kunz, "A frequency-dependent finite-difference time-domain formulation for transient propagation in plasma," *IEEE Trans. Antennas Propag.*, vol. 39, no. 1, pp. 29–34, Jan. 1991.
[21] L. J. Nickisch and P. M. Franke, "Finite-difference time-domain solution of Maxwell's equations for the dispersive ionosphere," *IEEE Antennas Propag. Mag.*, vol. 34, no. 10, pp. 33–38, Oct. 1992.
[22] J. L. Young, "A full finite difference time domain implementation for radio wave propagation in a plasma," *Radio Sci.*, vol. 29, no. 6, pp. 1513–1522, Nov.–Dec. 1994.
[23] J. L. Young and F. P. Brueckner, "A time domain numerical model of a warm plasma," *Radio Sci.*, vol. 29, no. 2, pp. 451–463, 1994.
[24] J. L. Young and R. O. Nelson, "A summary and systematic analysis of FDTD algorithms for linearly dispersive media," *IEEE Antennas Propag. Mag.*, vol. 43, pp. 61–77, Feb. 2001.
[25] R. W. Schunk and A. F. Nagy, *Ionospheres Physics, Plasma Physics, and Chemisty*, ser. Cambridge Atmospheric and Space Science Series. New York: Cambridge Univ. Press, 2000.
[26] K. S. Kunz and R. J. Luebbers, *The Finite Difference Time Domain Method for Electromagnetics*. Boca Raton, FL: CRC Press, 1993.
[27] S. Berntsen and S. N. Hornsleth, "Retarded time absorbing boundary conditions," *IEEE Trans. Antennas Propag.*, vol. 42, no. 8, pp. 1059–1064, Aug. 1994.
[28] G.-X. Fan and Q. H. Liu, "An FDTD algorithm with perfectly matched layers for general dispersive media," *IEEE Trans. Antennas Propag.*, vol. 48, no. 5, pp. 637–646, May 2000.
[29] J. F. Olakangil, "FDTD model of plasma," master's thesis, Utah State Univ., Logan, 2000.
[30] R. C. Johnson, Ed., *Antenna Engineering Handbook*, 3rd ed. New York: McGraw-Hill, 1993.
[31] T. Ishizone, S. Adachi, K. Taira, Y. Mushiake, and K. Miyazaki, "Measurement of antenna current distribution in an anisotropic plasma," *IEEE Trans. Antennas Propag.*, vol. AP-17, no. 5, pp. 678–679, Sep. 1969.
[32] E. F. Pound, private communication Personal communications.
[33] ——, "Techniques to improve electron density measurements in the D region of the ionosphere," Ph.D. dissertation, Utah State Univ., Logan, 1995.

Jeffrey Ward (S'98) was born in 1972. He received the B.S. degree from Brigham Young University, Provo, UT, in 1997 and the M.S. degree from Utah State University, Logan, in 2002, both in electrical engineering. He is currently working toward the Ph.D. degree at Utah State University.

His research interests include antennas and plasma diagnostics.

Charles Swenson (M'84) was born in 1962. He received the B.S. and M.S. degrees from Utah State University, Logan, in 1985 and 1989, respectively, and the Ph.D. degree from Cornell University, Ithaca, NY, in 1992, all in electrical engineering.

He is an Associate Professor of electrical and computer engineering with Utah State University, Logan. His research activities are with the Space Dynamics Laboratory, where he is working on diagnostic instrumentation for space science and small satellite systems engineering.

Cynthia Furse (M'84–SM'99) received the Ph.D. degree from the University of Utah, Salt Lake City, in 1994.

She is the Director of the Center of Excellence for Smart Sensors at the University of Utah and an Associate Professor in the Electrical and Computer Engineering Department where she teaches electromagnetics, wireless communication, computational electromagnetics, microwave engineering, and antenna design. She has directed the Utah "Smart Wiring" program, sponsored by NAVAIR and USAF, since 1998.

Dr. Furse was Professor of the Year in the College of Engineering, Utah State University, in 2000; Faculty Employee of the Year in 2002; a National Science Foundation Computational and Information Sciences and Engineering Graduate Fellow; a IEEE Microwave Theory and Techniques Graduate Fellow; and President's Scholar at the University of Utah. She is the Chair of the IEEE Antennas and Propagation Society Education Committee and an Associate Editor of the IEEE TRANSACTIONS ON ANTENNAS AND PROPAGATION.